JOURNAL OF CATALYSIS 99, 278–292 (1986)

Studies of the Interactions of H_2 and CO with Pd/SiO_2 Promoted with La_2O_3, CeO_2, Pr_6O_{11}, Nd_2O_3, and Sm_2O_3

JEFFERY S. RIECK AND ALEXIS T. BELL

Materials and Molecular Research Division, Lawrence Berkeley Laboratory; and Department of Chemical Engineering, University of California, Berkeley, California 94720

Received August 19, 1985; revised January 3, 1986

The interactions of H_2 and CO with Pd/SiO_2 promoted with La_2O_3, CeO_2, Pr_6O_{11}, Nd_2O_3, and Sm_2O_3 have been investigated using temperature-programmed desorption and temperature-programmed surface reaction. Introduction of the promoter following the preparation of the Pd/SiO_2 catalyst results in a partial coverage of the Pd particles by the oxide promoter. Upon reduction of the promoted catalysts, portions of the promoter in contact with Pd undergo reduction. The partially reduced rare earth oxide species covering the Pd particles reduce the amounts of H_2 and CO that can be adsorbed on the metal. The rare earth oxide moieties have a slight influence on the distribution of H_2 adstates but cause a significant change in the distribution of CO adstates. Decoration of Pd by rare earth oxide moieties also aids the dissociation of CO, and raises thereby the activity for CH_4 synthesis relative to that for Pd/SiO_2. The promoter also serves to increase the activity for CH_3OH synthesis and the formation of CO_2 via the water-gas shift reaction. © 1986 Academic Press, Inc.

INTRODUCTION

The activity and selectivity of Pd for CO hydrogenation depend in a complex fashion on Pd dispersion, crystallite morphology, and support composition; however, the observations of different investigators do not always agree. Ichikawa *et al.* (*1*) and Doering *et al.* (*2, 3*) have reported that the turnover frequency for methanation over Pd/SiO_2 increases with Pd dispersion. On the other hand, Rieck and Bell (*4*) and Hicks and Bell (*5*) have observed the opposite effect for Pd/SiO_2 and Pd/La_2O_3. Hicks and Bell (*5*) found no effect of Pd dispersion on the turnover frequency for methanol formation over Pd/SiO_2 or Pd/La_2O_3, provided the particle morphology did not change. These authors noted, however, that the turnover frequency for methanol synthesis was nearly threefold greater on particles exposing (100) facets rather than (111) facets, thereby emphasizing the importance of Pd crystallite morphology.

The influence of support composition on the catalytic properties of Pd has also been examined by a number of authors (*5–26*). High methanation activity and selectivity is achieved by supporting Pd on TiO_2 or ZrO_2. On the other hand, high activity and selectivity for methanol synthesis can be achieved by use of La_2O_3 or Nd_2O_3 as the support (*5–14*). Studies aimed at understanding the effects of support composition (*21–26*) have revealed that these effects appear to be due in large measure to the decoration of the supported Pd crystallites by metal oxide moieties derived from the support. The validity of this interpretation has recently been supported by studies demonstrating that Pd/SiO_2 promoted with TiO_2 or La_2O_3 exhibits adsorptive and catalytic properties virtually identical to those observed when Pd is supported on these oxides (*25, 26*). Additional evidence for the decoration model comes from the observation of changes in the catalytic activity and selectivity of Pd/SiO_2 promoted with MgO or alkali metal oxide (*14, 17, 24, 27*).

In the present paper we report on experiments aimed at understanding the interactions of H_2 and CO with Pd/SiO_2 promoted

0021-9517/86 $3.00

with La_2O_3, CeO_2, Pr_6O_{11}, Nd_2O_3, and Sm_2O_3. The advantage of using the rare earth oxide as a promoter rather than as a support is that it allows the Pd dispersion to be kept constant, and as a consequence removes one of the variables influencing the properties of Pd. The principal techniques used in this study were temperature-programmed desorption (TPD), temperature-programmed reduction (TPR), and temperature-programmed surface reaction (TPSR).

EXPERIMENTAL

Apparatus

The apparatus used for the present study has been described previously (*28–30*). The catalysts were placed in a quartz microreactor which could be heated at up to 1 K/s. The desorbing gas was swept from the microreactor by a continuous flow of carrier gas. Analysis of the effluent flow was performed with a quadrupole mass spectrometer. The transfer time from the microreactor to the mass spectrometer was less than 1.5 s. A microprocessor-based data acquisition system was used to direct the mass spectrometer to a series of preselected masses and to record the signal intensity at each mass setting. The catalyst temperature was also recorded by the data acquisition system.

Materials

The methods of catalyst preparation and characterization employed have been described previously (*26*, *31*, *32*). The 2% Pd/SiO_2 was obtained by incipient wetness impregnation of Cab-O-Sil HS-5 silica with a solution of H_2PdCl_4 dissolved in 1 *N* HCl. This catalyst was dried and calcined in a 21% O_2/He mixture at 623 K for 2 h.

The rare earth oxide-promoted Pd/SiO_2 catalysts were prepared in a manner identical to that used previously to prepare lanthana-promoted Pd/SiO_2 (*25*). A portion of the calcined 2% Pd/SiO_2 catalyst was impregnated with a solution of the rare earth nitrate in deionized H_2O and dried. The catalysts were calcined again to decompose the nitrate precursor and reduced in H_2 at the desired reduction temperature. The loadings of the rare earth oxides correspond to a ratio of rare earth metal to surface Pd atoms of 5.0. These catalysts were characterized using H_2–O_2 titration.

Helium and H_2 were purified to remove O_2 and water; and CO was purified to remove metal carbonyls, water, and CO_2. Details of the purification procedures are given in Ref. (*26*). The absence of impurities in these gases was established by mass spectrometry.

Experimental Procedure

The experimental procedures used in this study are similar to those described in Ref. (*26*). A mass of catalyst corresponding to 3.8×10^{-6} mol of surface palladium atoms based on H_2–O_2 titration was placed in the microreactor. The mass and the particle size were selected to avoid inter- and intraparticle mass transfer effects (*33*). The catalysts were reduced in H_2 at temperatures ranging from 523 to 673 K. Following pretreatment, adsorption was performed by pulsing or flowing the desired gases through the catalyst bed. For temperature-programmed desorption (TPD) and temperature-programmed surface reaction (TPSR) experiments, flow rates of 50 cm^3/min of He and H_2 were used, respectively. The heating was 1 K/s for these experiments. The relative activities of the catalysts for CO hydrogenation were determined by ramping the catalyst temperature at 1 K/s in a flow of 75 cm^3/min of H_2 and 25 cm^3/min of CO. For temperature-programmed reduction (TPR) experiments, the catalyst was calcined, and then the temperature was ramped at 0.25 K/s in a flow of 200 cm^3/min of 1000 ppm H_2 in He. For temperature-programmed oxidation (TPO) experiments, the catalyst temperature was ramped at 0.25 K/s in a flow of 200 cm^3/min of 1000 ppm O_2 in He, following reduction. Following each experiment, the mass spectrometer was calibrated against He mixtures containing specified concentrations of H_2 and CO.

The absolute rates of desorption are based on the number of surface Pd atoms present calculated from H_2–O_2 titration. The moles of gas desorbing during an experiment were calculated by first integrating the spectra to find the peak areas, and then multiplying by the proper calibration factor. The initial coverages were found by dividing the number of moles desorbed by the moles of surface Pd present based on H_2–O_2 titration.

RESULTS

H_2–O_2 Titration

The dispersions of the catalysts based on H_2–O_2 titration are given in Table 1. For 2% Pd/SiO_2, this value agrees with that determined previously (*30*) by H_2 or CO chemisorption. The H_2–O_2 titration results show that the rare earth oxide-promoted Pd/SiO_2 catalysts have the same dispersion as Pd/SiO_2, independent of the reduction temperature.

Temperature-Programmed Reduction and Oxidation

TPR and TPO experiments were performed to characterize the reducibility of 2% Pd/SiO_2 and the promoted catalysts. The uptakes of H_2 and O_2 are summarized in Table 2. Also listed are the differences

TABLE 1

Pd Dispersion of Pd/SiO_2 and Rare Earth Oxide-Promoted Pd/SiO_2

Catalyst	Dispersion[a] (%)	
	573 K	673 K
2% Pd/SiO_2	35	34
4.4% La/(2% Pd/SiO_2)	35	34
4.4% Ce/(2% Pd/SiO_2)	33	32
4.4% Pr/(2% Pd/SiO_2)	33	32
4.5% Nd/(2% Pd/SiO_2)	32	33
4.7% Sm/(2% Pd/SiO_2)	33	33

[a] Based on H_2–O_2 titration. Temperatures are T_{red}.

TABLE 2

H_2 and O_2 Uptakes Observed during TPR and TPO

Catalyst[a]	H_2 consumption at 298 K ($\times 10^{-6}$ mol)	H_2 consumption during TPR ($\times 10^{-6}$ mol)	Excess H_2 consumption over Pd/SiO_2 ($\times 10^{-6}$ mol)	O_2 consumption at 298 K[b] ($\times 10^{-6}$ mol)	Excess O_2 consumption over Pd/SiO_2 ($\times 10^{-6}$ mol)
2.0% Pd/SiO_2	0	13.0	—	2.70	—
4.4% La/(2% Pd/SiO_2)	4.20	9.47	0.67	3.5	0.80
4.4% Ce/(2% Pd/SiO_2)	5.73	8.04	0.77	3.18	0.48
4.4% Pr/(2% Pd/SiO_2)	4.36	9.32	0.68	3.22	0.52
4.5% Nd/(2% Pd/SiO_2)	2.20	11.03	0.23	2.97	0.27
4.7% Sm/(2% Pd/SiO_2)	4.15	9.62	0.77	3.3	0.60

[a] Surface Pd: 3.81×10^{-6} mol. Bulk Pd: 1.09×10^{-5} mol.

[b] No O_2 uptake during TPO.

between the uptakes by the promoted and unpromoted samples of 2% Pd/SiO_2. For the sake of comparison, the total amount of Pd present based on H_2–O_2 titration are listed at the bottom of the table. For 2% Pd/SiO_2, the spectrum for H_2 consumption during TPR consists of single peak at 343 K. The spectra for the promoted catalysts exhibit a peak at 320–325 K, and the peaks for La_2O_3- and Pr_6O_{11}-promoted Pd/SiO_2 have high-temperature shoulders at 368 and 373 K, respectively. As shown in Table 2, the total H_2 consumption for each promoted sample is greater than that for Pd/SiO_2. The TPO experiments revealed that the catalysts consumed of O_2 at room temperature. The O_2 consumption by each promoted catalyst was greater than that for Pd/SiO_2. However, there was no further uptake of O_2 during the temperature ramp.

H_2 and CO TPD

The TPD spectra for H_2 desorption from 2% Pd/SiO_2 and the five promoted catalysts are shown in Fig. 1. The initial coverage by adsorbed H atoms, θ_H°, is based on the amount of H_2 desorbed up to 873 K. For 2% Pd/SiO_2, the saturation coverage is 1.03. Although the promoted catalysts have the same dispersion based on H_2–O_2 titration, the chemisorption capacity of these catalysts is less than that of unpromoted Pd/SiO_2. The reduction in H_2 chemisorption capacity increases in the order: $Sm_2O_3 < CeO_2 < Nd_2O_3 < Pr_6O_{11} < La_2O_3$. No change in the saturation coverages was observed when the reduction temperature was increased from 523 to 673 K.

Figure 1 shows that promotion of Pd/SiO_2 with rare earth oxides results in subtle changes in the distribution of adstates for H_2 chemisorption. As shown in Fig. 1, the major peak for H_2 desorption from 2% Pd/SiO_2 is located at 470 K. This peak is accompanied by an unresolved high-temperature shoulder between 540 and 570 K. The shape of the spectrum indicates another peak is present on the low-temperature side. Figure 1 shows that, following promotion with La_2O_3, Sm_2O_3, or Nd_2O_3, the major peak for H_2 desorption is still located at 470–480 K. However, the spectra for Sm_2O_3- and Nd_2O_3-promoted Pd/SiO_2 exhibit a well-resolved low-temperature peak at 390–400 K. Following promotion with Pr_6O_{11}, the major peak occurs at 445 K, again with a shoulder at 390 K. After promotion with CeO_2, the major peak for desorption occurs at 410 K, and the peak at 470 K becomes a high-temperature shoulder. The shapes of the desorption spectra for the promoted samples indicate that the higher-temperature peak at 540–570 K is still present, although it is smaller in magnitude. Thus, there is a general suppression of all H_2 adstates.

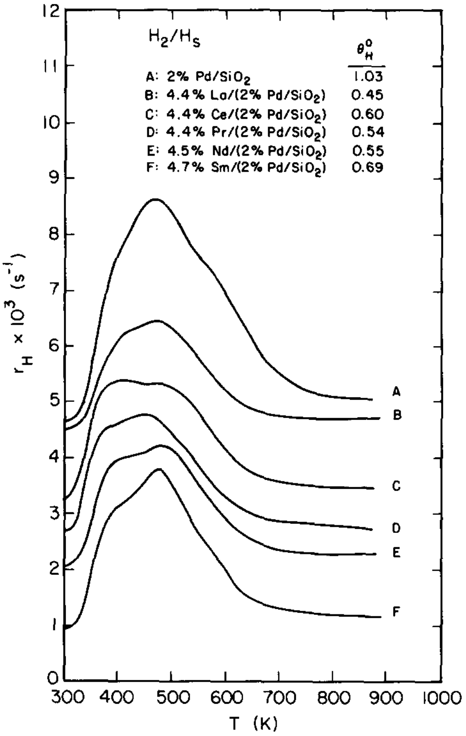

FIG. 1. Effects of rare earth oxide promotion on the H_2 TPD spectra for 2% Pd/SiO_2. Note that spectra have been offset for clarity.

The CO desorption spectra for 2% Pd/SiO_2 and rare earth oxide-promoted Pd/SiO_2 are shown in Fig. 2a. The spectra for the CO_2 evolved during CO desorption are

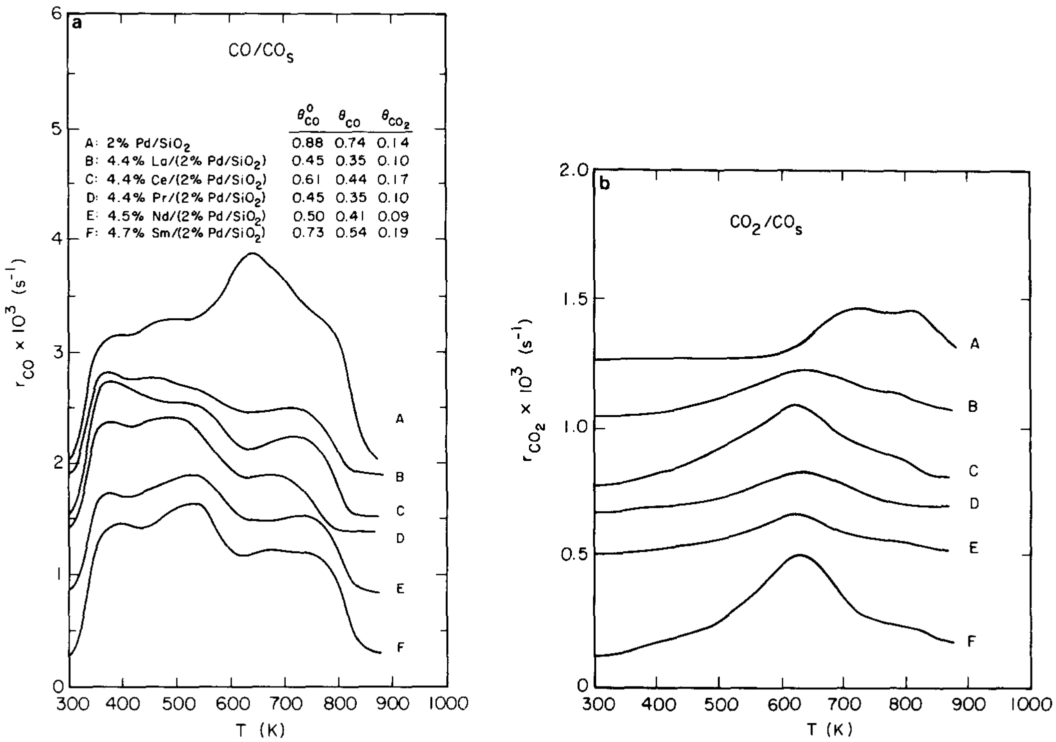

FIG. 2. Effects of rare earth oxide promotion on the desorption products observed during CO TPD from 2% Pd/SiO$_2$: (a) CO: (b) CO$_2$. Note that spectra have been offset for clarity.

given in Fig. 2b. Since no H_2 was observed during the CO TPD experiments, the water-gas-shift reaction can be ruled out as the source of the CO_2. Therefore, the CO_2 formed can be attributed totally to the disproportionation of CO: 2 $CO_{ads} \rightarrow C_{ads} + CO_2$. The initial coverage of CO, θ^0_{CO}, given in Fig. 2a is taken to be the amount of CO desorbed, θ_{CO}, plus twice the amount of CO_2 produced. The equivalent coverage of CO converted to CO_2 is given by θ_{CO_2}.

The spectrum for CO TPD from 2% Pd/SiO$_2$ shown in Fig. 2a consists of four peaks located at 400, 488, 638, and 773 K. The saturation coverage is 0.88. As shown in Fig. 2a, promotion with the rare earths results in a suppression of the initial CO uptake. The magnitude of this suppression follows the same trend with promoter as observed for H_2 adsorption. However, in contrast to the results given in Fig. 1 for H_2 desorption, the spectra for CO desorption show that promotion with rare earth oxides causes a significant redistribution in the forms of adsorbed CO. For all of the promoted samples, there is a preferential suppression of the peaks at 638 and 773 K. In addition, promotion with CeO_2 of La_2O_3 results in a suppression of the peak at 488 K. For all five promoted catalysts, the suppression of the peak at 400 K is quite small. No change in amount of CO adsorbed nor the distribution of adstates was observed upon increasing the reduction temperature from 523 to 673 K.

Figure 2b shows that all six catalysts produced significant amounts of CO_2 during CO TPD. CO_2 formation is observed over 2% Pd/SiO$_2$ at temperatures above 570 K and reaches a maximum rate at 735 K. The onset of CO_2 formation over the promoted catalysts occurs at much lower temperatures, between 350 and 380 K. The peak locations for maximum CO_2 production are also shifted to lower temperatures, ranging from 620 to 640 K. Thus, the promotion of Pd/SiO_2 with a rare earth oxide induces CO dissociation at lower temperatures. The quantity of CO_2 produced was also altered by rare earth oxide promotion. The fraction of initially adsorbed CO which dissociates during TPD increases in the order: unpromoted (8%) < Nd_2O_3 (9%) < La_2O_3 (11%) = Pr_6O_{11} (11%) < Sm_2O_3 (13%) < CeO_2 (14%).

The reversibility of the suppression of CO chemisorption caused by rare earth oxide promotion was investigated in the following manner. A reduced Nd_2O_3-promoted Pd/SiO_2 sample was saturated with O_2 at 298 K, and the adsorbed oxygen was titrated with H_2. The uptake of CO was then measured. It was observed that CO displaced the adsorbed H_2, and the catalyst chemisorbed 0.65 of a monolayer of CO, compared to the saturation coverage of 0.50 shown in Fig. 2 for a reduced sample. The subsequent TPD yielded little useful information since the H_2O present resulted in a large CO_2 feature due to the water-gas-shift reaction. However, it is significant that exposing the catalyst to O_2 resulted in an increase in its chemisorption capacity.

TPSR of H_2 and CO

TPSR experiments were performed on the promoted catalysts to gain further information regarding the influence of the rare earth oxides on the catalyst performance. The methane features for the TPSR of CO following adsorption at room temperature are given in Fig. 3a for 2% Pd/SiO_2 and the five promoted catalysts. The spectra for CO desorption during the TPSR are given in Fig. 3b. The initial coverages by CO, θ^{0}_{CO}, are in good agreement with those shown in Fig. 2 for CO TPD. The methane spectrum for 2% Pd/SiO_2 exhibits a single peak at 620 K. Promotion with the rare earth oxides results in a large shift in the peak for methane production to lower temperatures. The peak locations increase in the order: Nd_2O_3 (517 K) = CeO_2 (517 K) < Sm_2O_3 (522 K) <

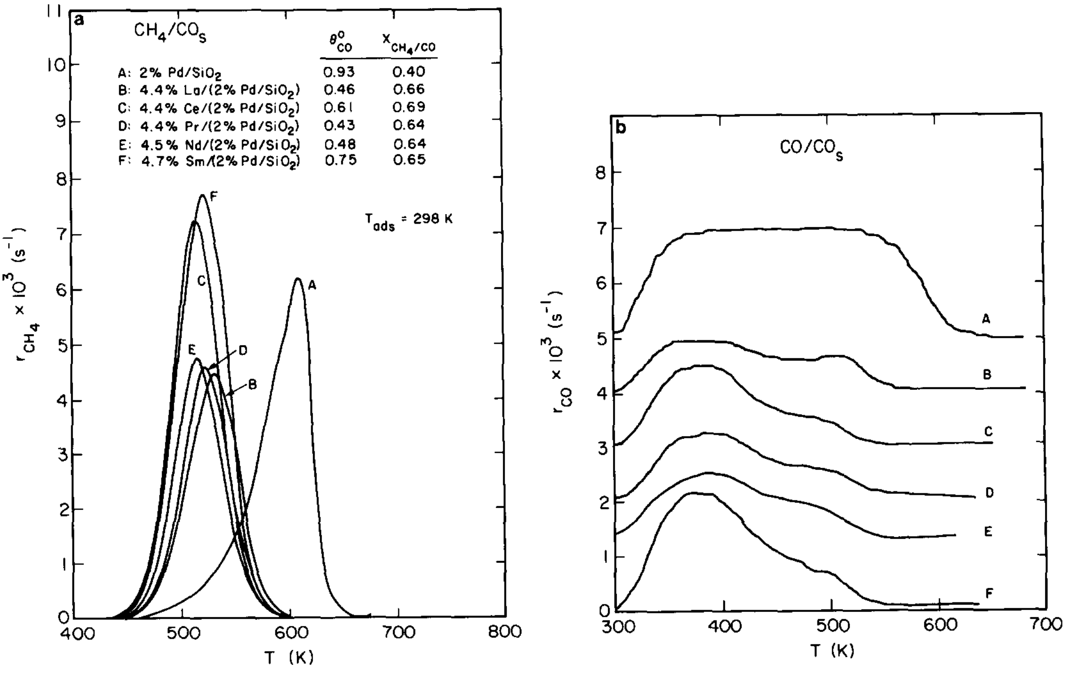

FIG. 3. Effects of rare earth oxide promotion on the products formed during TPSR of CO adsorbed on 2% Pd/SiO_2: (a) CH_4; (b) CO. Note that spectra have been offset for clarity.

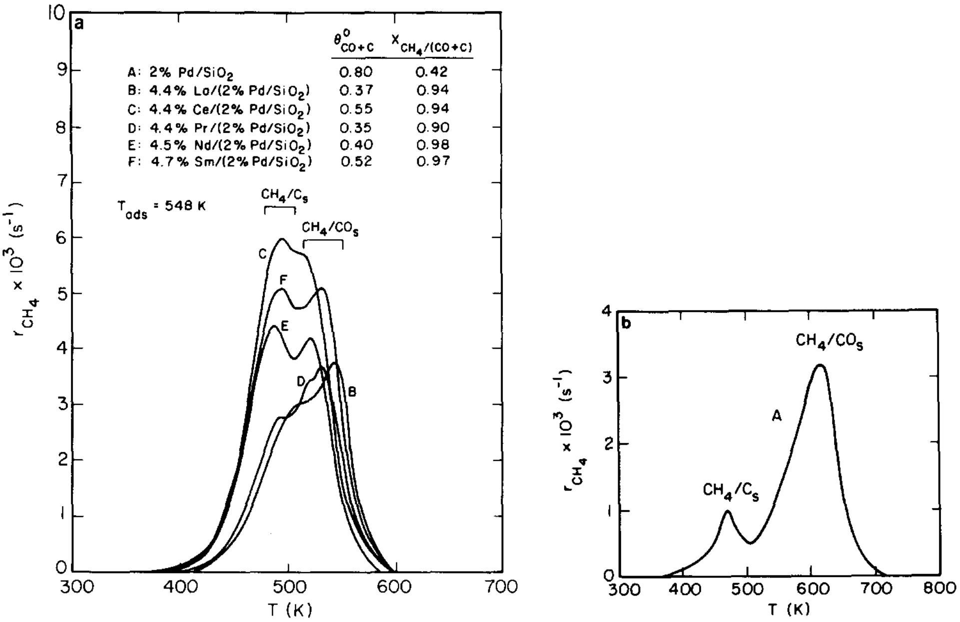

FIG. 4. Effects of CO adsorption at 548 K on CH_4 formation during TPSR of CO adsorbed on: (a) rare earth oxide-promoted Pd/SiO_4; (b) 2% Pd/SiO_2.

Pr_6O_{11} (525 K) < La_2O_3 (533 K). The fraction of initially adsorbed CO which reacts to give CH_4, $X_{CH_4/CO}$, is 0.40 for 2% Pd/SiO_2. This quantity increases for the promoted catalysts to between 0.64 and 0.69. Thus, the promotion of Pd/SiO_2 with a rare earth oxide significantly increases its activity for the hydrogenation of molecular CO.

The effects of rare earth oxide promotion on the activity of Pd/SiO_2 for CO dissociation were investigated by performing the TPSR experiments following CO adsorption at elevated temperatures. Figure 4a shows the CH_4 produced by the promoted catalysts during the TPSR of CO adsorbed at 548 K. The CH_4 spectrum for the TPSR of CO adsorbed at 548 K on 2% Pd/SiO_2 is shown in Fig. 4b. For 2% Pd/SiO_2, a low temperature peak is observed at 475 K along with a peak at 630 K. This low-temperature peak is attributed to the hydrogenation of surface carbon deposited during the adsorption step (*25*). For this adsorption temperature, only 0.06 of a monolayer of surface carbon is deposited. In addition, a large amount of CO desorbs unreacted. The spectra in Fig. 4a reveal that, following CO adsorption at 548 K, the promoted catalysts exhibit much larger peaks due to the methanation of surface carbon. Very little unreacted CO desorbs, since $X_{CH_4/(CO+C)}$ is very close to 1.0 for the promoted samples. Thus, the promotion of Pd/SiO_2 with a rare earth oxide results in a much higher activity for CO dissociation. CeO_2- and Nd_2O_3-promoted Pd/SiO_2 exhibit the highest activity for CO dissociation, while that of Sm_2O_3-promoted Pd/SiO_2 is slightly lower. The dissociation activities of La_2O_3- and Pr_6O_{11}-promoted Pd/SiO_2 are, however, significantly lower.

The CH_4 spectra for the TPSR of CO adsorbed at 623 K on the promoted catalysts are shown in Fig. 5. The spectra consist of a peak from the hydrogenation of surface carbon and a high temperature shoulder from the hydrogenation of the residual CO left on the surface after adsorption. For all five catalysts, no unreacted CO was observed during the TPSR. The spectrum for TPSR

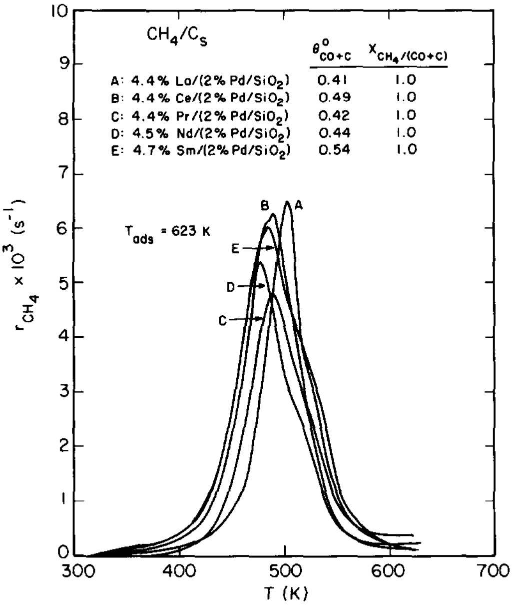

FIG. 5. Effects of CO adsorption at 623 K on CH_4 formation during TPSR of CO adsorbed on rare earth oxide-promoted Pd/SiO_2.

of CO adsorbed at 673 K on 2% Pd/SiO_2 produced a peak from the hydrogenation of surface carbon at 473 K (*25*). Thus, it is seen from the peak locations that the relative reactivities of the surface carbon decreases in the order: unpromoted (473 K) > Nd_2O_3 (478 K) > Sm_2O_3 (485 K) > CeO_2 (489 K) = Pr_6O_{11} (489 K) > La_2O_3 (503 K). These experiments also give evidence of the high activity of the promoted catalysts for CO dissociation. During the adsorption of CO at 673 K, only 0.32 of a monolayer of carbon is deposited on 2% Pd/SiO_2 (*26*). Figure 5 shows that the amount of carbon deposited on all of the promoted catalysts is greater than 0.40 of a monolayer for an adsorption temperature of only 623 K.

The influence of H_2 on the dissociation of CO was investigated by adsorbing CO at 498 K in the presence of 10% H_2. Figure 6a shows the CH_4 formation over the promoted catalysts during TPSR following such an adsorption step. The CH_4 spectra

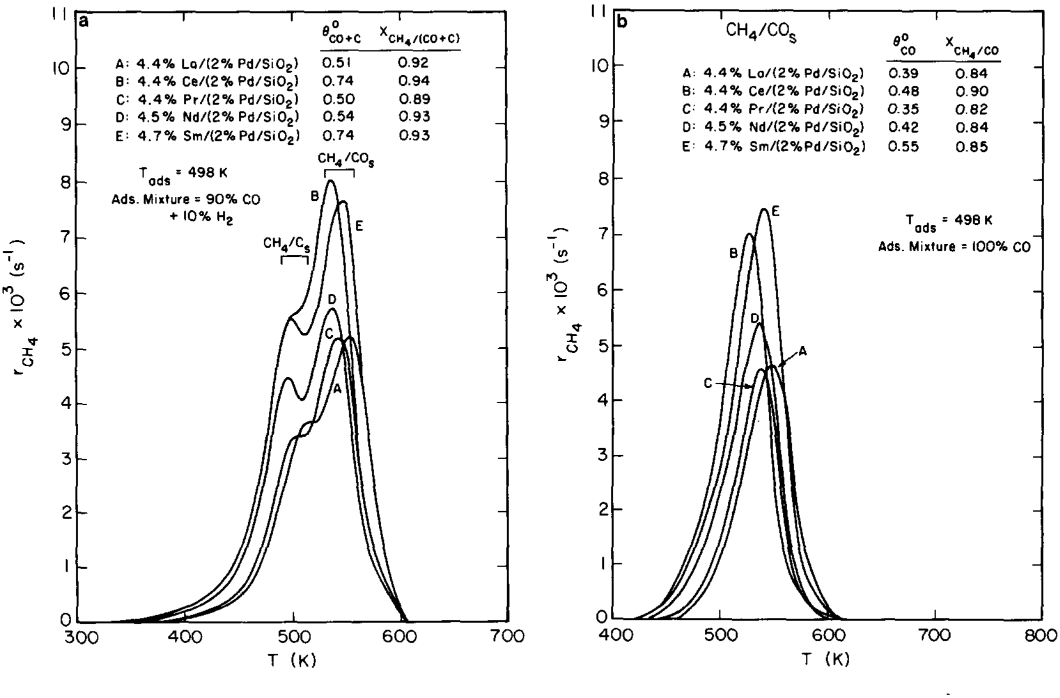

FIG. 6. Effects of the presence of H_2 during CO adsorption on CH_4 formation during TPSR for rare earth oxide-promoted Pd/SiO_2: (a) adsorption mixture = 90% CO, 10% H_2; (b) adsorption mixture = 100% CO.

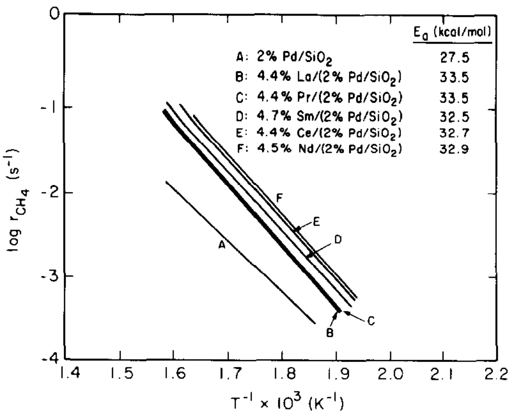

FIG. 7. Comparison of the activities of Pd/SiO_2 and rare earth oxide-promoted Pd/SiO_2 for CH_4 production; $P = 1$ atm, $H_2/CO = 3/1$.

for TPSR following the adsorption of CO at 498 K in the absence of H_2 are shown in Fig. 6b for comparison. After adsorption of pure CO at 498 K, there is no evidence for the presence of a peak due to the hydrogenation of surface carbon. However, Fig. 6a shows that all five promoted catalysts exhibit a prominent peak for the hydrogenation of carbon after the adsorption of CO in the presence of H_2. Thus, as seen with Pd/SiO_2 (*25*), the presence of H_2 results in a buildup of carbon on the catalysts. As was shown in Fig. 4 for the adsorption of pure CO at 548 K, the La_2O_3- and Pr_6O_{11}-promoted Pd/SiO_2 catalysts have a lower activity for CO dissociation in the presence of H_2 than the other promoted catalysts. However, the quantity of carbon deposited in the presence of H_2 at 498 K on the promoted catalysts is much larger than the amount deposited on Pd/SiO_2 for the same adsorption conditions, 0.09 of a monolayer (*26*).

Comparison of Activities for CO Methanation

The dependence of the methanation activity of each catalyst on temperature was determined by raising the catalyst temperature at 1 K/s in a flowing mixture of synthesis gas. In all cases, the maximum conversion was kept below 1%. An Arrhenius plot for CH_4 production, basing the number of active sites on H_2–O_2 titration, is given in Fig. 7. The catalyst activities increase in the following order: unpromoted < La_2O_3 < Pr_6O_{11} < Sm_2O_3 < CeO_2 < Nd_2O_3. The activation energies for methanation are given in Fig. 7. The lowest value of E_a is 27.5 kcal/mol, for 2% Pd/SiO_2. The activation energies for the promoted catalysts are very similar, ranging between 32.5 and 33.5 kcal/mol.

The Arrhenius plot in Fig. 8 shows the CO_2 production observed during methanation. The activities for CO_2 production increase in the order: Nd_2O_3 < La_2O_3 < Sm_2O_3 < Pr_6O_{11} < CeO_2. Pd/SiO_2 produced only trace amounts of CO_2. Comparison of Figs. 7 and 8 shows that the rate of methane production is greater than the rate of CO_2 production for all of the catalysts throughout the temperature range. The activation energies for CO_2 production are shown in Fig. 8. These range between 20.7 and 22.0 kcal/mol. Due to its low activity for CO_2 production, the activation energy could not be calculated for Pd/SiO_2.

Small quantities of CH_3OH were formed over the promoted catalysts as shown in Fig. 9. The variation in methanol synthesis activity with promoter follows the trend:

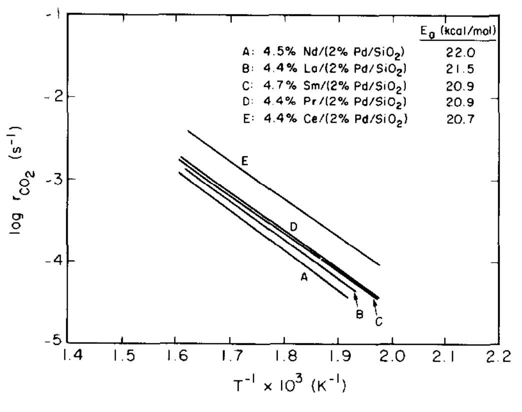

FIG. 8. Comparison of the activities of Pd/SiO_2 and rare earth oxide-promoted Pd/SiO_2 for CO_2 production; $P = 1$ atm, $H_2/CO = 3/1$.

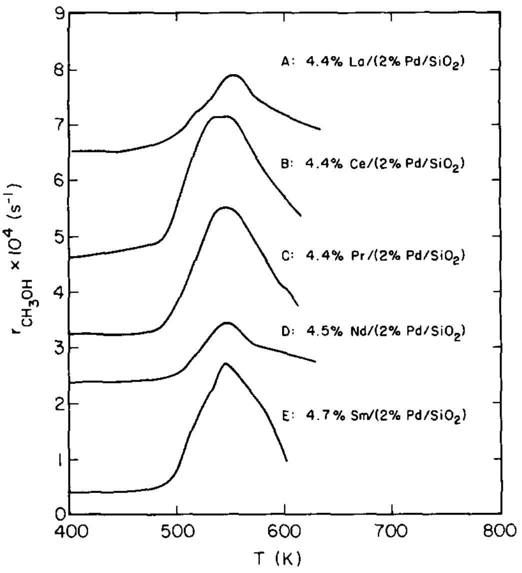

FIG. 9. Comparison of the activities of Pd/SiO_2 and rare earth oxide-promoted Pd/SiO_2 for CH_3OH production; P = 1 atm, H_2/CO = 3/1. Note plots have been offset for clarity.

$Nd_2O_3 < La_2O_3 < Sm_2O_3 < CeO_2 = Pr_6O_{11}$. No methanol was produced over 2% Pd/SiO_2. Variation of the reduction temperature between 523 and 673 K had no influence on either the activity or the selectivity of the catalysts.

DISCUSSION

H_2–O_2 Titration

The results of H_2–O_2 titration presented in Table 1 clearly demonstrate that the dispersion of silica-supported Pd is virtually unchanged by promotion with rare earth oxides. Moreover, the dispersion is the same for reduction temperatures of 573 and 673 K. Similar observations have also been reported for La_2O_3- and TiO_2-promoted Pd/SiO_2 (*25*, *26*). It is quite significant to observe that the moles of exposed Pd determined by H_2–O_2 titration is quite different from that which would be determined by H_2 or CO chemisorption, the latter two methods always yielding lower values. These differences are ascribed to the influence of adsorbate composition on the degree of wetting of the Pd surface by the oxide promoter. Following reduction, the Pd particles are in their metallic state and the rare earth oxide in contact with the particles is slightly deficient in oxygen. This deficiency in oxygen contributes to an improved wetting of the metal by the promoter and blockage of adsorption sites. Thus, when H_2 or CO is adsorbed on a reduced Pd/SiO_2 sample that has been promoted, the adsorbate uptake is always less than that measured for unpromoted Pd/SiO_2. On the other hand, if a promoted catalyst undergoes a sequence of O_2–H_2 titrations, following reduction, the exposure to O_2 causes a reoxidation of the promoter. This process, in turn, presumably causes a reduction in the extent of wetting and hence an increase in the amount of Pd surface atoms exposed. As a consequence, H_2–O_2 titration results in a measure of all surface Pd atoms. The data in Table 1 demonstrate further that the procedure used to add the rare earth oxide promoter does not influence the dispersion of Pd.

TPR and TPO

The amount of H_2 consumed during TPR and the shape of the spectra for H_2 consumption can provide evidence for the reduction of catalyst supports and promoters. The results of TPO experiments indicate the degree of reversibility of the reduction. As shown in Table 2, each sample contains 1.09×10^{-5} mol of total Pd and 3.81×10^{-6} mol of surface Pd. During the reduction of 2% Pd/SiO_2, 1.3×10^{-5} mol of H_2 is consumed. This uptake corresponds to reduction of bulk PdO and adsorbed surface oxygen. The uptake of 2.7×10^{-6} mol of O_2 during TPO can be ascribed to the reaction

$$Pd_s\text{—}H + \tfrac{3}{4}\,O_2 \rightarrow Pd_s\text{—}O + \tfrac{1}{2}\,H_2O$$

Bulk oxidation of Pd does not occur due to the low concentration of O_2 in the oxidizing stream. Thus, for Pd/SiO_2, only the Pd crystallites undergo oxidation and reduction.

The results of the TPR and TPO experiments for promoted Pd/SiO_2 give evidence for reduction of the rare earth oxide promoter. Only the spectra for La_2O_3- and Pr_6O_{11}-promoted Pd/SiO_2 exhibit a well-resolved TPR peak in addition to that corresponding to reduction of the Pd, which may be attributed to reduction of the promoter. However, the uptakes of H_2 shown in Table 2 demonstrate that all the promoted catalysts consumed H_2 in excess of that necessary to reduce the Pd. This excess consumption is attributed to reduction of the rare earth oxide promoter. The TPO results demonstrate that the O_2 uptakes on the promoted catalysts are also in excess of that observed for Pd/SiO_2. The excess O_2 consumption is attributed to the reoxidation of the reduced rare earth oxide. It is significant to note, though, that the amount of O_2 consumed corresponds to less than 5% of the oxygen present in the original oxide. A further point to note is that in all instances the amount of excess O_2 exceeds 0.5 times the amount of excess H_2. A possible reason for this is that there are anionic defects present in the promoter prior to TPR and that these, plus the additional defects formed during TPR, are removed during TPO.

H_2 TPD

The spectra for H_2 desorption in Fig. 1 shows that the chemisorption of H_2 is suppressed on the rare earth oxide-promoted catalysts. However, the degree of suppression is not a function of the reduction temperature. This indicates that, in contrast to the behavior of TiO_2-promoted catalysts (*26*), the extent of adsorption site blockage by the promoter does not increase with increasing reduction temperature.

In addition to the suppression of H_2 chemisorption, the spectra show that the energetics of H_2 desorption are slightly altered by rare earth oxide promotion. For all of the promoted catalysts, the peak at 470 K on 2% Pd/SiO_2 is more strongly suppressed relative to the other peaks. Due to the suppression of this peak, the peak at 390–400 K becomes better resolved. However, there are no major shifts in the distribution of adstates for H_2 adsorption. The results presented here agree well with those for TiO_2-promoted Pd/SiO_2 for which it was also observed that the energetics of H_2 desorption are not significantly different from those for Pd/SiO_2 (*26*).

CO TPD

The rare earth oxide-promoted catalysts exhibit a suppression in the degree of CO chemisorption similar to that seen for H_2 chemisorption. This result agrees with studies of TiO_2-promoted Pd/SiO_2 performed by Rieck and Bell (*26*), and with studies of TiO_2-supported noble metals in general (*34, 36*). Static chemisorption studies performed by Hicks *et al.* (*31*) on Pd/La_2O_3 indicated that the chemisorption of CO was more strongly suppressed than that of H_2. However, the chemisorption studies of Hicks *et al.* (*31*) do not allow the discrimination between H_2 adsorbed on Pd metal and H_2 adsorbed either on the bulk support or the REO_x moieties decorating the Pd particles. Thus, it is possible that the high H_2 uptakes observed by Hicks *et al.* (*31*) resulted from adsorption on the support.

The TPD spectrum for CO desorption from 2% Pd/SiO_2 is comprised of four peaks centered at 400, 488, 638, and 773 K. By comparing CO TPD results with the infrared studies of Hicks *et al.* (*31*), Rieck and Bell (*25*) attributed the peaks at 638 and 773 K to CO bridge bonded on Pd(100) and Pd(111) planes, respectively. The two low-temperature peaks were assigned to linearly adsorbed CO. Promotion of Pd/SiO_2 with a rare earth oxide results in a drastic change in the distribution of adstates for CO adsorption. As shown in Fig. 2, the peaks at 638 and 773 K are much more strongly attenuated than the two low-temperature peaks. In addition, the spectra for the La_2O_3- and CeO_2-promoted samples show that the peak at 488 K is more strongly suppressed than on the other three promoted samples. Thus, it appears that the structure of the partially reduced rare earth oxide patches decorating the Pd particles results in a preferential blockage of adsorption sites for bridge-bonded CO, but there is no preferential suppression of adsorption onto a specific crystal plane. This contrasts the results for TiO_2-promoted Pd/SiO_2, for which the peak corresponding to CO bridge-bonded to Pd(100) planes was preferentially suppressed (*26*).

Rieck and Bell (*25*) demonstrated for La_2O_3-promoted Pd/SiO_2 that the presence of La_2O_3 results in a higher activity for CO dissociation. The present study shows that this effect is observed for rare earth oxide promotion in general. The downscale shift in the peak position for CO_2 production over the promoted catalysts indicates that these catalysts have a higher activity for CO dissociation. This effect is attributed to the decoration of the surfaces of the Pd particles with rare earth oxide moieties. The participation of metal oxide moieties in promoting the dissociation of CO on Group VIII metals has been proposed recently by a number of authors (*13, 21, 22, 25, 36–38*). It is suggested that cations or oxygen vacancies in metal oxide moieties covering the supported metal particles interact with the oxygen end of CO molecules adsorbed on the metal. A possible scheme for this interaction is shown below.

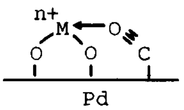

M^{n+}= Rare earth cation

TPSR of Adsorbed CO

The formation of CH_4 from CO over Pd is believed to proceed via the dissociation of CO (*18, 26*). Previous studies by Rieck and Bell (*25, 26*) of Pd/SiO_2, TiO_2-promoted Pd/SiO_2, and La_2O_3-promoted Pd/SiO_2 have shown that the carbon formed by the predissociation of CO on these catalysts is much more easily hydrogenated than molecular CO. This supports the premise that CO dissociation is the rate-limiting step for methanation. As noted above, rare earth oxide promotion of Pd/SiO_2 facilitates the dissociation of CO. This explains the TPSR results of Fig. 3a. The lower peak temperatures for methane formation for the rare earth oxide-promoted Pd/SiO_2 results from the participation of promoter moieties in the dissociation of CO. While the exact nature of the dissociation step is not known, it is clear from Figs. 6a and b that the dissociation of CO occurs more readily in the presence of H_2. This supports the idea of H-assisted CO dissociated proposed by Wang *et. al.* (*16*). A similar effect of H_2 has also been observed by Rieck and Bell (*26*) for Pd/SiO_2 and TiO_2-promoted Pd/SiO_2, and by Niizuma *et al.* (*39*) for Pd/Al_2O_3.

In addition to affecting the dissociation of CO, the decoration of Pd with rare earth oxide moieties alters the reactivity of adsorbed carbon. Rieck and Bell (*25*) reported a peak temperature of 473 K for the hydrogenation of carbon adsorbed on Pd/SiO_2. Figure 5 shows that the peak temperature for hydrogenation of adsorbed carbon increases with rare earth oxide promotion, with a maximum shift of 20 K for La_2O_3-promoted Pd/SiO_2. Since the kinetics of carbon hydrogenation are first-order in carbon coverage (*40, 41*), this shift indicates that the carbon is less reactive. However, since all five promoted catalysts exhibit a higher methanation activity than Pd/SiO_2, it must be concluded that the enhanced dissociation of adsorbed CO dominates the reduction in carbon reactivity.

While several recent studies (*1–5*) have shown that Pd dispersion influences the specific activity of Pd for methanation, such effects play no role in the present study since the Pd dispersion was the same for all catalysts. Consequently, the differences in specific activity was observed in Fig. 7 can be attributed exclusively to the influence of the promoter. It is important to recall that the specific activities reported in this figure are all based on measurements of exposed Pd determined by H_2–O_2 titration.

This procedure is to be preferred over that involving the use of exposed metal determined by H_2 or CO chemisorption on a reduced catalyst. The reason is as follows. *In situ* infrared spectra of Pd/La_2O_3 have shown that while a suppression in the chemisorption of CO can be observed at the beginning of CO hydrogenation, the coverage by adsorbed CO slowly increases and approaches a monolayer (*5*). This suggests that the water produced in conjunction with methane causes a reoxidation of the oxide moieties covering the Pd particles and, hence, a reduction in their ability to wet the Pd particle surface. Similar effects have also been reported for Pd/TiO_2 (*26*). In view of this, we believe that in its working state only a small fraction of the Pd particle surfaces may be covered by rare earth oxide promoter and, hence, that the specific activity calculations should be based on the total number of Pd surface atoms, and not just those exposed following catalyst reduction.

The trends in the methanation activities shown in Fig. 7 are consistent with the TPSR results. The two most active catalysts for methanation, Nd_2O_3- and CeO_2-promoted Pd/SiO_2, exhibited the highest dissociation activity, as shown by Fig. 4a. Since the carbon adsorbed on Nd_2O_3-promoted Pd/SiO_2 is more reactive than that adsorbed on CeO_2-promoted Pd/SiO_2 (see Fig. 5), the Nd_2O_3-promoted catalysts exhibits a slightly higher methanation activity. The promoted catalysts exhibiting the lowest activity for methanation, La_2O_3- and Pr_6O_{11}-promoted Pd/SiO_2, are also the least active for CO dissociation. Since the carbon adsorbed on the La_2O_3-promoted catalyst is less reactive than that on the Pr_6O_{11}-promoted catalyst, this is the least active methanation catalyst.

It is of interest to draw a comparison between the observations of this study with those reported by Vannice and co-workers (*11, 13*) for CO hydrogenation over the rare earth oxide supported Pd. There is general agreement that the presence of rare earth oxides, either a support or promoter, increases the specific activity of Pd for ethanation by over a factor of 10 relative to the activity observed for Pd/SiO_2. The principal differences are in the ranking of the effectiveness of the oxides. Thus, for example, our work indicates that Nd_2O_3-promoted Pd/SiO_2 is the most active catalyst, while Mitchell and Vannice (*11*) find Pd/Pr_6O_{11} and Sudhakar and Vannice (*13*) find Pd/CeO_2 to be the most active catalysts. The differences reported by different authors may be due to differences in Pd dispersions for the different rare earth oxide supported catalysts and to differences in the degree of Pd decoration by oxidic moieties by different rare earth oxides.

The activation energies shown in Fig. 7 for methanation over the rare earth oxide-promoted catalysts range between 32.5 and 33.5 kcal/mol, while that for Pd/SiO_2 is 27.5 kcal/mol. This agrees well with studies by Hicks and Bell (*12*) and Rieck and Bell (*25*) which have shown that the activation energy for methanation over Pd/La_2O_3 is greater than that over Pd/SiO_2, and with the work of Underwood and Bell (*42*) in which the activation energies for methanation over Rh/La_2O_3, Rh/Sm_2O_3, and Rh/Nd_2O_3 are found to be higher than over Rh/SiO_2. Mitchell and Vannice (*11*), on the other hand, have reported that the activation energies for methanation over Pd supported on rare earth oxides range between 19.9 and 32.4 kcal/mol following reduction at 448 K, and between 21.6 and 30.4 kcal/mol following reduction at 773 K. No clear explanation was given for the wide range of activation energies nor for the dependence of activation energy on catalyst reduction temperature. In the work of Sudhakar and Vannice (*13*), catalyst reduction was carried out only at 773 K, and the activation energies for methane formation ranged between 31.2 and 33.7 kcal/mol.

The higher activation energies for methane formation over rare earth oxide-promoted Pd/SiO_2 relative to unpromoted Pd/SiO_2 contrasts with what has been observed for TiO_2-promoted Pd/SiO_2 (*26*). In this latter case, the activation energy is 3 kcal/mol lower for the promoted catalyst. Thus, unlike TiO_2-promoted Pd/SiO_2, the higher activity of rare earth oxide-promoted Pd/SiO_2 cannot be attributed to an overall reduction in reaction energetics. This is somewhat surprising in view of the fact that Fig. 2b shows that promotion with a rare earth oxide lowers the temperature at which CO dissociates to produce carbon. From these observations, we are led to conclude that the rare earth oxide moieties on Pd create a large number of sites at which CO dissociation can occur but that the energetics associated with these sites are less favorable than those present on Pd itself. By contrast, TiO_2 promotion may form active sites at which the energetics are more favorable than those for unpromoted Pd. This would explain why comparable methanation activities require roughly tenfold less moles of promoter when TiO_2 rather than a rare earth oxide is used.

The formation of only a small amount of methanol, relative to methane, over the promoted catalysts is not surprising since all of the activity studies reported here were carried out at atmospheric pressure. Previous investigations with Pd catalysts have shown that the selectivity to methanol is greatly enhanced as the pressure is increased (*11, 18*). Nevertheless, the fact that methanol formation is enhanced by the addition of a rare earth oxide again points to the ability of such oxides to activate adsorbed CO.

The results presented in Fig. 8 demonstrate that in addition to enhancing the rates of formation of methane and methanol, promotion of Pd/SiO_2 with rare earth oxide results in the formation of CO_2, a product not observed over unpromoted Pd/SiO_2. The presence of CO_2 can be ascribed to the promotion of the water-gas shift reaction brought about by the promoter. Mitchell and Vannice (*11*) also observed the production of CO_2 over Pd supported on rare earth oxides. However, in contrast to the present study, the specific rates of CO_2 formation always exceeded the formation of methane. Mitchell and Vannice (*11*) attributed this to the decomposition of carbonate structures formed on the support.

The activation energy for CO_2 formation observed here is approximately 21 kcal/mol, varying little with the composition of the promoter. This value can be compared with the data of Mitchell and Vannice (*11*), who measured activation energies ranging between 12 and 29 kcal/mol for Pd supported on rare earth oxides. It is also significant to note that while Mitchell and Vannice observed a decrease in the activation energy for CO_2 formation when catalyst reduction was carried out at 773 K instead of at 448 K, no change in the activation energy was observed in studies reported here.

CONCLUSIONS

The promotion of Pd/SiO_2 with a rare earth oxide results in a modification of the adsorptive and catalytic properties of Pd. These changes are attributed to the decoration of Pd particles by partially reduced rare earth oxide moieties. These species result in a suppression in H_2 and CO chemisorption. The distribution of H_2 adstates is not significantly changed, but the distribution of CO adstates is strongly affected. Adsorption of CO into strongly held states is greatly suppressed, and the dissociation of CO is facilitated. While the carbon formed via CO dissociation reacts more readily with H_2 to form methane than does adsorbed CO, the reactivity of adsorbed carbon is slightly less for promoted than unpromoted Pd/SiO_2.

The specific activity of Pd/SiO_2 for methanation increases by as much as 12-fold when promoted with a rare earth oxide, the highest specific activity being observed for Nd_2O_3-promoted Pd/SiO_2. The higher activity of the rare earth oxide promoted catalysts is accompanied, though, by a higher activation energy. This suggests that the higher activity of the promoted catalysts is due to a higher concentration of catalytically active sites, than that present on the unpromoted catalyst. Since the hydrogenation of CO to CH_4 is believed to proceed via the dissociation of adsorbed CO, it is inferred that promotion of Pd with a rare earth oxide increases the number of CO dissociation sites but that the activation energy for CO dissociation may, in fact, increase relative to that for unpromoted Pd. In addition to increasing the specific activity for methanation, promotion of Pd/SiO_2 with a rare earth oxide also increases the specific activities for methanol synthesis and the formation of CO_2 via the water-gas shift reaction.

ACKNOWLEDGMENT

This work was supported by the Division of Chemical Sciences, Office of Basic Energy Sciences, U.S. Department of Energy under Contract DE-AC03-76SF00098.

REFERENCES

1. Ichikawa, S., Poppa, H., and Boudart, M., *J. Catal.* **91,** 1 (1985).
2. Doering, D. L., Poppa, H., and Dickinson, J. T., *J. Catal.* **73,** 104 (1982).
3. Doering, D. L., Poppa, H., and Dickinson, J. T., *J. Vac. Sci. Technol.* **17,** 198 (1980).
4. Rieck, J. S., and Bell, A. T., submited for publication.
5. Hicks, R. F., and Bell, A. T., *J. Catal.* **90,** 205 (1984).
6. Ichikawa, M., *Shokubai* **21,** 253 (1979).
7. Poels, E. K., van Broekhoven, E. H., van Barneveld, W. A. A., and Ponec, V., *React. Kinet. Catal. Lett.* **18,** 223 (1981).
8. Ryndin, Yu. A., Hicks, R. F., Bell, A. T., and Yermakov, Yu. I., *J. Catal.* **70,** 287 (1981).
9. Ponec, V., *Stud. Surf. Sci. Catal.* **11,** 63 (1982).
10. Poels, E. K., Koolstra, R., Geus, J. W., and Ponec, V., *Stud. Surf. Sci. Catal.* **11,** 233 (1982).
11. Mitchell, M. D., and Vannice, M. A., *Ind. Eng. Chem. Fundam.* **23,** 88 (1984).
12. Hicks, R. F., and Bell, A. T., *J. Catal.* **91,** 104 (1984).
13. Sudhakar, C., and Vannice, M. A., *J. Catal.* **95,** 227 (1985).
14. Vannice, M. A., *J. Catal.* **40,** 129 (1975).
15. Vannice, M. A., and Garten, R. L., *Ind. Eng. Chem. Prod. Res. Dev.* **18,** 186 (1979).
16. Wang, S.-Y., Moon, S. H., and Vannice, M. A., *J. Catal.* **71,** 167 (1981).
17. Kikuzono, Y., Kagami, S., Naito, S., Onishi, T., and Tamaru, K., *Faraday Discuss. Chem. Soc.* **72,** 135 (1982).
18. Fajula, F., Anthony, R. G., and Lunsford, J. H., *J. Catal.* **73,** 237 (1982).
19. Driessen, J. M., Poels, E. K., Hindermann, J. P., and Ponec, V., *J. Catal.* **82,** 26 (1983).
20. Yoshioka, H., Naito, S., and Tamaru, K., *Chem. Lett.*, 981 (1983).
21. Bracey, J. D., and Burch, R., *J. Catal.* **86,** 384 (1984).
22. Anderson, J. B. F., Bracey, J. D., Burch, R., and Flambard, A. R., *in* "Proceedings, 8th International, Congress on Catalysis, Vol. V, p. 111. Berlin, 1984.
23. Kunimori, K., Abe, H., Yamaguchi, E., Matsui, S., and Uchijima, T., *in* Proceedings, 8th International Congress on Catalysis," Vol. V, p. 251. Berlin, 1984.
24. Kelly, K. P., Tatsumi, T., Uematsu, T., and Lunsford, J. H., *J. Catal.*, in press.
25. Rieck, J. S., and Bell, A. T., *J. Catal.* **96,** 88 (1985).
26. Rieck, J. S., and Bell, A. T., *J. Catal.* **99,** 262 (1986).
27. Rieck, J. S., and Bell, A. T., in press.
28. Low, G., and Bell, A. T., *J. Catal.* **57,** 397 (1979).
29. Uchida, M., and Bell, A. T., *J. Catal.* **60,** 204 (1979).
30. Chin, A. A., and Bell, A. T., *J. Phys. Chem.* **87,** 3700 (1983).
31. Hicks, R. F., Yen, Q.-J., and Bell, A. T., *J. Catal.* **89,** 498 (1984).
32. Fleisch, T. H., Hicks, R. F., and Bell, A. T., *J. Catal.* **87,** 398 (1984).
33. Rieck, J. S., and Bell, A. T., *J. Catal.* **85,** 143 (1984).
34. Tauster, S. J., Fung, S. C., and Garten, R. L., *J. Amer. Chem. Soc.* **100,** 170 (1978).
35. Vannice, M. A., *J. Catal.* **74,** 199 (1982).
36. Vannice, M. A., and Sudhakar, C., *J. Phys. Chem.* **88,** 2429 (1984).
37. Sachtler, W. M. H., *in* "Proceedings, 8th International Congress on Catalysis," Vol. V, p. 151. Berlin, 1984.
38. Sachtler, W. M. H., Shriver, D. F., Hollenberg, W. B., and Long, A. F., *J. Catal.* **92,** 429 (1985).
39. Niizuma, H., Hattori, T., Mori, T., Miyamoto, A., and Murakami, Y., *J. Phys. Chem.* **87,** 3652 (1983).
40. Winslow, P., and Bell, A. T., *J. Catal.* **86,** 154 (1984).
41. Ozdogan, S. Z., Gochis, P. D., and Falconer, J. L., *J. Catal.* **83,** 257 (1983).
42. Underwood, R. P., and Bell, A. T., *Appl. Catal.*, in press.